Epizootic of Clinostomum marginatum (Trematoda: Clinostomidae) in Ambystoma tigrinum from Colorado, USA: Investigation through Genomics, Histopathology, and Noninvasive Imagery

Article *in* Journal of Wildlife Diseases · March 2025

DOI: 10.7589/JWD-D-24-00068

CITATION
1

READS
40

6 authors, including:

Dana M Calhoun
University of Colorado Boulder
45 PUBLICATIONS **639** CITATIONS
SEE PROFILE

Jasmine Groves
University of Colorado Boulder
1 PUBLICATION **1** CITATION
SEE PROFILE

Tyler Achatz
Middle Georgia State University
43 PUBLICATIONS **387** CITATIONS
SEE PROFILE

Stephen Greiman
Georgia Southern University
92 PUBLICATIONS **1,096** CITATIONS
SEE PROFILE

EPIZOOTIC OF CLINOSTOMUM MARGINATUM (TREMATODA: CLINOSTOMIDAE) IN AMBYSTOMA TIGRINUM FROM COLORADO, USA: INVESTIGATION THROUGH GENOMICS, HISTOPATHOLOGY, AND NONINVASIVE IMAGERY

Authors: Calhoun, Dana M., Groves, Jasmine, Schaffer, Paula A., Achatz, Tyler J., Greiman, Stephen E., et al.

Source: Journal of Wildlife Diseases, 61(2) : 448-460

Published By: Wildlife Disease Association

URL: https://doi.org/10.7589/JWD-D-24-00068

DOI: 10.7589/JWD-D-24-00068

Journal of Wildlife Diseases, 61(2), 2025, pp. 448–460

Epizootic of *Clinostomum marginatum* (Trematoda: Clinostomidae) in *Ambystoma tigrinum* from Colorado, USA: Investigation through Genomics, Histopathology, and Noninvasive Imagery

Dana M. Calhoun,[1,5] Jasmine Groves,[1] Paula A. Schaffer,[2] Tyler J. Achatz,[3] Stephen E. Greiman,[4] and Pieter T.J. Johnson[1]

[1] Ecology and Evolutionary Biology, University of Colorado, Boulder, Colorado 80309, USA
[2] Microbiology, Immunology, and Pathology, Veterinary Diagnostic Laboratories, Colorado State University, Fort Collins, Colorado 80521, USA
[3] Department of Natural Sciences, Middle Georgia State University, Macon, Georgia 31206, USA
[4] Department of Biology, Georgia Southern University, Statesboro, Georgia 30460, USA
[5] Corresponding author (email: dana.calhoun@colorado.edu)

ABSTRACT: Trematodes in the genus *Clinostomum* develop into large metacercariae that can sometimes achieve high intensity in their second intermediate hosts, potentially causing pathology. In 2022, there was 100% (15/15) infection prevalence of *Clinostomum marginatum*, with a mean of 3,125 metacercariae per salamander (range: 279–4,075) and a median of 2,949. Dissection and histopathology results indicated that *C. marginatum* was found in nearly all body tissues and organs of the salamanders. Parasitic infection was closely associated with chronic inflammation and fibrosis around the cysts, with heavily infected hosts exhibiting altered buoyancy and difficulty swimming. The following summer, only 22.0% (6/27) of salamanders were infected with *C. marginatum*; based on their size, these were probably overwintering larvae from 2022. Here, we characterize a morbidity event in tiger salamanders (*Ambystoma tigrinum*) from a freshwater pond in Boulder, Colorado, USA, linked to extreme clinostomid infection. After using necropsy, genomic analysis, and histopathological assessment to record the intensity and pathology associated with infections, we assessed the validity of using noninvasive, image-based methods to quantify infection. Over 2 yr, we recorded in situ video imagery of 62 larval *A. tigrinum*, of which a subset of larvae was collected for parasitological assessment. Infection loads of *C. marginatum* quantified indirectly via imagery of subcutaneous cysts correlated strongly with direct counts via necropsy and were consistent between independent reviewers, highlighting the utility of this non-invasive assessment method. All evaluated *A. tigrinum* were co-infected with additional parasite taxa. Prevalence of other trematodes included *Ribeiroia ondatrae* (80%) and *Cephalogonimus americanus* (77.5%), as well as the nematode *Megalobatrachonema elongata* (75%). To discern the impact of such high metacercarial burden of *C. marginatum* on tiger salamander, future work should incorporate experimental approaches to evaluate load-dependent consequences for host growth, survival, behavior, and time to metamorphosis.

Key words: Epizootic, salamander morbidity, trematode pathology, concurrent infection.

INTRODUCTION

Pathogen-induced population declines and extinction events have been increasingly recognized as important threats to amphibian species around the globe (Daszak et al. 2003; Blaustein et al. 2012; Bower et al. 2019). Fungal pathogens such as *Batrachochytrium dendrobatidis* (Bd) and *Batrachochytrium salamandrivorans* (Bsal) have been linked with at least 500 amphibian species declines and extinctions (Olson et al. 2013; Becker et al. 2016; Scheele et al. 2019). Infections by ranaviruses, which have been detected in at least 105 species of amphibians, have also been linked to die-offs in temperate climates (Green et al. 2002; Gray et al. 2009; Duffus et al. 2015). More recently, studies have detailed complex interactions among several factors (e.g. disease, environmental contamination, climate change, etc.) that may negatively affect amphibians in nature (Herczeg et al. 2021). For instance, tadpoles of the midwife toads, *Alytes obstetricans*, exposed to microplastics demonstrated an increase in Bd zoospore load (Bosch et al. 2021), potentially limiting osmoregulation through the skin and increasing the risk of cardiac arrest. Further investigations are needed to understand the consequences of these interactions for individual amphibian health as well as population persistence.

Nevertheless, many amphibian mortality or morbidity events often go unreported or incompletely characterized.

Alongside fungal and viral microparasites, amphibians host a wide variety of macroparasites, such as trematodes, cestodes, and nematodes. These are commonly detected, but tend to cause pathology only when infection loads are very high. For example, Cururu toads (*Rhinella icterica*) in Brazil infected with high loads of the lung nematode *Rhabdias fuelleborni* demonstrated reduced locomotor performance (Moretti et al. 2014), and *Rhabdias bufonis* has been shown to inhibit growth and survival of European toads (*Bufo bufo*) and wood frogs (*Rana sylvatica*; Goater and Ward 1992; Goater et al. 1993; Goater and Vandenbos 1997). Despite the ubiquity of macroparasite infections in amphibians, detecting and quantifying the consequences of such infections in amphibian host populations is notoriously difficult (Wilber et al. 2020). One reason for this is that the effects of macroparasite infections are often sublethal, altering host growth, behavior, and reproductive rates (Hudson and Greenman 1998; Albon et al. 2002; Koprivnikar et al. 2012). For example, wood frog (*R. sylvatica*) tadpoles exposed to the trematode *Echinostoma trivolvis* cercariae over time decreased their growth and increased developmental time—a critical time for the frogs, as they are vulnerable to predators (Orlofske et al. 2017).

Because of the threatened status of many amphibians, developing noninvasive methods to investigate morbidity or mortality events represents an important strategy to advance understanding while limiting adverse consequences. Noninvasive techniques used to detect pathogens in amphibians include antigen or molecular detection applied to samples from live animals or their environments (DiRenzo et al. 2018; Everest et al. 2019; Schilling et al. 2022). Analysis of fecal samples is one of the most common and widely used approaches for parasite detection (Luikart et al. 2006). For pathogens evident in the skin or mucosal tissues, swabbing of hosts followed by genomic screening has been widely applied to detect and quantify infections by pathogens such as Bd and Bsal (Standish et al. 2018). Such approaches can be complemented by the use of environmental DNA (eDNA) to detect evidence of pathogens in water or soil samples (Huver et al. 2015; Kolby et al. 2015; Hall et al. 2018). Use of high-resolution imagery can further assist in assessing infections that form conspicuous lesions or other externally apparent signs of infection (e.g., host behavioral changes). De Wit and Johnson (2024) used video transects to survey >5,000 reef fishes for skin lesions associated with Black Spot Syndrome caused by the trematode *Scaphanocephalus* spp.

We characterized a morbidity event in tiger salamanders (*A. tigrinum*) from Boulder, Colorado, US, associated with exceptionally high loads of infection by *Clinostomum marginatum.* Trematodes in the genus *Clinostomum* have been reported in anurans and urodeles worldwide (McAllister 1990; Calhoun et al. 2019). Freshwater snails serve as the first intermediate hosts, and many species of fish and amphibians act as second intermediate hosts (Calhoun et al. 2019). *Clinostomum* spp. adults are found in fish-eating birds, reptiles, and occasionally mammals, including humans. Although *Clinostomum* spp. have rarely been associated with reports of pathology of clinical relevance and morbidity, infection by large numbers *Clinostomum* spp. induced scoliosis in a tiger salamander (*Ambystoma tigrinum*) in the US (Perpiñán et al. 2010). Our objective was to use necropsy, morphological and genomic analysis, and histopathology to quantify infection intensity and characterize the pathology associated with infections. We also aimed to compare infection load determined by necropsy with estimates generated through video imaging to determine whether the load of *Clinostomum* metacercariae could be noninvasively estimated in live animals, which could enable expansion of the role of community science in data collection during amphibian epizootics.

FIGURE 1. Blue Stem Connector Pond in Boulder, Colorado, USA. Inset: an *Ambystoma tigrinum* found in the pond in 2022, which was lethargic, with numerous 1–2-mm-diameter raised white dermal nodules.

MATERIALS AND METHODS

Field collections and necropsy

During a routine field visit to a freshwater pond (Blue Stem Connector Pond, 39°57′33.5514″N, 105°15′39.492″W) in Boulder, Colorado, in August 2022, we observed an *A. tigrinum* that was extremely lethargic, emaciated, and unable to maintain proper buoyancy. The individual was extensively covered with elevated, white to yellow dermal nodules (mean dermal size 1.65 ± 0.07 μm; n=10) consistent with parasitic infection (Fig. 1). The salamander did not evade or resist capture. Gross necropsy and subsequent microscopy confirmed clinostomid infection. Specifically, *Clinostomum* spp. metacercariae can be identified by a stout body, oral sucker surrounded by a collar that is similar in size when compared to the ventral sucker, and a bulbous esophagus with little to no pharynx (Schell 1985; Hoffman 1999; Caffara et al. 2011). Clinostomid metacercariae can be large, conspicuously colored either white or yellow, and tend to be mobile when escaped from their cyst in fresh hosts (Calhoun et al. 2019). The pond was revisited multiple times to investigate the infection pattern. From August 2022 to May 2023, *A. tigrinum* were collected using a combination of dip nets (D-frame with 1.2-mm mesh), seines (1.2 × 1.8 m), and hand capture (Johnson et al. 2019). Each individual was carefully examined and video recorded (10–20-s duration) across the entire body surface to detect lesions. A randomly selected subset of individuals was collected to quantify infection via necropsy in accordance with permits from Boulder Open Space & Mountain Parks (OSMP) and Colorado Parks and Wildlife. Five additional infected salamanders were collected in 2022 and deposited in the University of Colorado Museum of Natural History (UCM 69089).

Salamanders were euthanized using buffered MS-222 (1 g/500 mL of water), measured using digital calipers (snout–vent length and total length), and dissected using the following standard methods (Johnson et al. 2018). Specifically, under an Olympus SZX16 stereo dissecting microscope (Olympus Corporation, Tokyo, Japan), all major organs and tissues including the heart, liver, lungs (when present), esophagus, small and large intestine, rectum, stomach, tongue, mandible, kidneys, gills, gall bladder, spleen, fat bodies, reproductive organs, eyes, head, and brain were removed, shredded using two forceps, and compressed between two gridded Petri dishes. Large organs were cut into smaller parts before shredding. After organ removal, the body cavity and ear canals were examined and the skin removed from the underlying muscle using a scalpel blade then shredded. Front and hind limbs

were shredded while attached to the bone and then compressed between gridded Petri dishes. Isolated parasites were counted and identified using morphological characters (viewed at 60–200× magnification on an Olympus BX51 microscope; Olympus Corporation, Tokyo, Japan) with the aid of taxonomic keys (Lehmann 1954; Schell 1985; Gibson et al. 2002). Parasites were removed using glass pipettes and placed on glass slides with coverslips for initial identification on a compound scope. Trematodes were heat-killed and preserved in 70% ethanol for further morphological analysis or 95% ethanol for molecular analysis. Nematodes were cleared and examined in temporary mounts of lactophenol to aid in identification. The mean load for each parasite taxon was calculated as the total number of parasites divided by the number of dissected hosts; mean intensity was calculated as the total number of parasites divided by the number of infected hosts (Bush et al. 1997). The median was provided to highlight the distribution of infection. Two salamanders from 2022 were examined for *Clinostomum* spp. infection only, because of their state of decomposition.

Genomic analysis

Genomic DNA of trematodes was extracted following the protocol in Tkach and Pawlowski (1999). Fragments of the ITS regions (ITS1 + 5.8S+ITS2) and large ribosomal subunit (28S) ribosomal DNA (rDNA) were amplified by polymerase chain reaction (PCR). Amplification of the ITS region used the forward primer ITSf (5′-CGC CCG TCG CTA CTA CCG ATT G-3′) and reverse primer 300R (5′-CAA CTT TCC CTC ACG GTA CTT G-3′; Snyder and Tkach 2007; Littlewood and Olson 2014); the 28S fragment was amplified with the forward primer digL2 (5′-AAG CAT ATC ACT AAG CGG-3′) and reverse primer 1500R (5′-GCT ATC CTG AGG GAA ACT TCG-3′; Tkach et al. 2003). Each PCR was carried out in a total volume of 25 µL using One-Taq quick load PCR mix (New England Biolabs, Ipswich, Massachusetts, USA) with an annealing temperature of 53 C. The PCR products were purified with an Illustra ExoProStar PCR clean-up enzymatic kit (Cytiva, Marlborough, Massachusetts, USA) and cycle-sequenced using a BrightDye Terminator Cycle Sequencing Kit (MCLAB, South San Francisco, California, USA) with PCR primers. Sequencing reactions were purified using a BigDye Sequencing Clean Up kit (MCLAB) and run on an ABI 3500 Genetic Analyzer (Thermo Fisher Scientific, Waltham, Massachusetts, USA). Contiguous sequences were assembled using Sequencher 4.2 software (GeneCodes Corp., Ann Arbor, Michigan, USA). The newly generated sequences were deposited in GenBank.

Histology

Two euthanized salamanders (one male, one female) were preserved in 10% neutral-buffered formalin for histopathology. The ventral body wall was incised before immersion whole in 10% neutral buffered formalin for >48 h. Sections of skin with body wall, gill, lung, heart, stomach, intestine, kidney, ovary or testis, spleen, liver, and head/spine were routinely trimmed, processed, mounted onto microscope slides and stained with H&E for evaluation by light microscopy. The axial skeleton and limbs were decalcified for <12 h in Nitrical (StatLab, McKinney, Texas, USA), then sections of head, thoracic, and lumbar spine, tail, and limbs were randomly selected and processed to slides. Slides were reviewed by a board-certified veterinary anatomic pathologist.

Video processing

To quantify infection of clinostomids noninvasively, videos of each salamander were processed using Windows Media Player (Microsoft, Redmond, Washington, USA). Videos were paused and taken frame by frame throughout the counting process to ensure each body part was observed, including dorsal side, ventral side, tail, hindlimbs (left and right), forelimbs (left and right), and gills (left and right). Cysts (metacercariae) presented as white to yellow, spherical raised nodules approximately 1–2-mm diameter. After each body part was observed, counts were totaled into a singular host infection load. Note that this method is unable to capture infections not visible on the surface of the skin or through the tissue, such as those around or within internal organs. If a body part was difficult to see (e.g., salamander moving too much, video did not capture a specific body part, or not in frame), the count was marked as "NA" and a note was made explaining the circumstance.

We compared counts of parasite cysts from video-recorded hosts with the totals found during necropsy for 23 individual salamanders using a generalized linear model (GLM) with a negative

binomial distribution ('nbinom1'). Not all animals collected were included in this analysis, which only focused on hosts with data both from video recordings and necropsy. The response variable was the count of *C. marginatum* for each host determined by necropsy, with the count from the video as the predictor. Because visual inspection of our data indicated that this relationship was not linear, we further incorporated a quadratic term (i.e., the squared value of cyst counts from video) and used Akaike information criterion (AIC) values to compare between models with and without the quadratic term. Both predictor terms were scaled before inclusion in the models (using the 'scale' function in R). To evaluate the validity of the video-based quantification method further, we compared cyst counts between two independent reviewers for an additional 34 larval salamanders that were not necropsied, using a linear correlation analysis. All statistical analysis were performed in the program R version 4.3.1 (R Core Team 2022) using the statistical package 'glmmTMB' (Brooks et al. 2017).

RESULTS

Field collections and necropsy

We necropsied 39 premetamorphic larval (larger than stage 46; Harrison 1969) and three postmetamorphic *A. tigrinum* to quantify macroparasite infections: 14 premetamorphic and one postmetamorphic salamanders in 2022 (mean total length 174.4±13.4 mm), 25 premetamorphic larvae and two postmetamorphic individuals in 2023 (mean total length 177.1±5.9 mm). In 2022, infection prevalence and abundance of *C. marginatum* were both higher with 100% (15/15) of hosts infected and a mean of 3,125 (range: 279–4,075; median: 2,949) metacercariae per salamander. These animals were lethargic, thin, and had difficulty with buoyancy. In 2023, prevalence was 22% (6/27) with a mean load of 237.14 (range: 0–1,994; median: 0); all infected larvae had a similar body size. In heavily infected hosts, *C. marginatum* metacercariae were embedded in almost every organ and tissue of their hosts, such as the epidermis, dermis, internal organs, subcutaneous space, muscular tissue, oral cavity, and even between the vertebrae of the spine. Each metacercaria was large and often easily detected externally, forming 1–2-mm diameter, white nodular cysts in or under the skin of their hosts (Figs. 1 and 2). The most frequent location for *C. marginatum* was free within the coelomic cavity (49.5%; Fig. 2), followed by the head region, which included the gills, mandible, head, and tongue (22.0%).

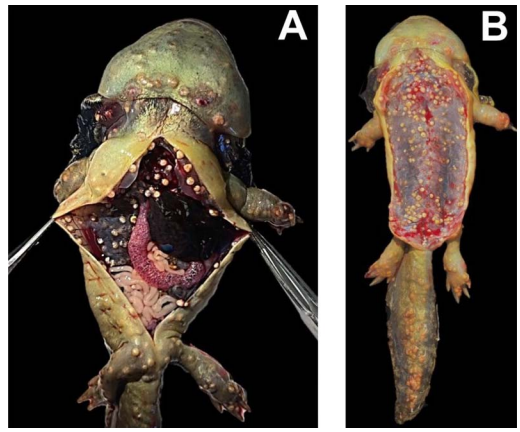

FIGURE 2. Gross examination of the 2022–2023 morbidity event in Colorado, USA, revealed severe infection loads of *Clinostomum marginatum* in *Ambystoma tigrinum* (total length 212.93 mm). (A) A larva opened along the midline with internal organs exposed; (B) a larva with the skin opened and the coelomic serosa still intact.

All dissected amphibians were infected with at least one parasite taxon and 95% were co-infected, although this varied by collection year (Fig. 3). In addition to *C. marginatum*, 47% of the salamanders collected in 2022 were also infected with metacercariae of the trematodes *Ribeiroia ondatrae* and *Cephalogonimus americanus,* although 27% were infected with four parasite taxa (*C. marginatum*, *R. ondatrae*, *Ce. americanus*, and the intestinal nematode *Megalobatrachonema elongata*). In 2023, only 22% of the salamanders were infected with *C. marginatum*; all individuals were co-infected with both *R. ondatrae* and *Ce. americanus.* The hosts not infected with *C. marginatum* were frequently infected with *Ce. americanus*, *R. ondatrae*, and the nematode *M. elongata.* Overall, 80% of hosts were infected with *R. ondatrae*, 77.5%

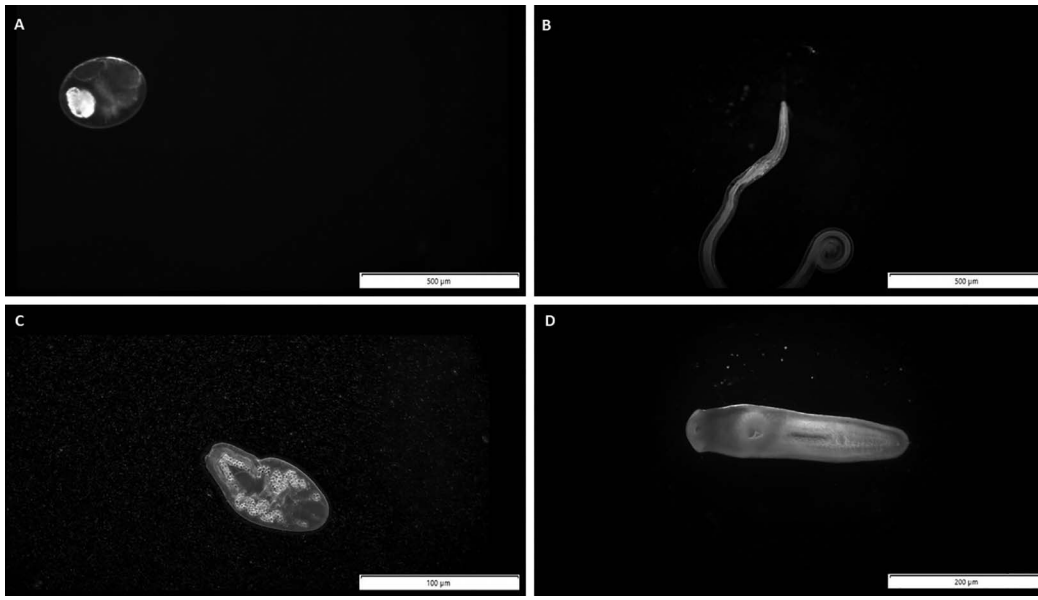

FIGURE 3. Microscopic images of helminths extracted from *Ambystoma tigrinum* from Blue Stem Connector Pond in Boulder, Colorado, USA, and placed on slides held by a coverslip. (A) metacercaria of *Cephalogonimus americanus*, (B) adult of *Megalobatrachonema elongata*, (C) metacercaria of *Ribeiroia ondatrae,* and (D) metacercaria of *Clinostomum marginatum.*

with *Ce. americanus* (adults and metacercariae), and 75% with adult *M. elongata.* Mean intensity ±1 SE and maximum loads for each parasite were as follows: *R. ondatrae*: 47.0±3.2, maximum load 98; *Ce. americanus* (adults and metacercariae): 57.6±15.3, maximum load 862; *M. elongata* 9.70±1.63; maximum load 48. *Ribeiroia ondatrae* and *Ce. americanus* metacercariae were detected primarily in the head region with high concentrations in the gills and gill reabsorption area (66.6%) as well as throughout the oral cavity (e.g., mandible and tongue; 20.6%). Both *Ce. americanus* adults (2.6±1.16) and the nematode *M. elongata* were found in the intestines in both collection years.

Genomic analysis

We generated three contiguous ITS region+28S sequences of *C. marginatum* (GenBank accessions PQ012242–PQ012244); these did not demonstrate any intraspecific variation. Based on a BLAST search, no differences were detected between our sequences and *C. marginatum* in GenBank, including those from a previous study by the several of the present authors (GenBank accessions MK424220–MK424227, MK424229, MK424230; Calhoun et al. 2019) and morphologically identified adult stages (e.g., GenBank accession KU708007). The single obtained sequence of *Ce. americanus* (GenBank accession PQ012240) and the sequence of *R. ondatrae* (GenBank accession PQ012241) also matched published sequences of morphologically identified adults (GenBank accessions HM137615 and KT956956), respectively (Razo-Mendivil and de León 2011; Tkach et al. 2016), which supported their identifications.

Histology

In the two salamanders prepared for histological analysis, *C. marginatum* metacercariae were found in the dermis or within the musculature deep to the skin (Fig. 4A). High infection intensity was identified in the submucosa of the gill rachis. More moderate numbers were present in the submucosa and muscularis of the stomach (Fig. 4B), and the interstitium associated with the testis, ovary, and oviduct. Metacercariae were less frequent in other visceral sites, with only occasional

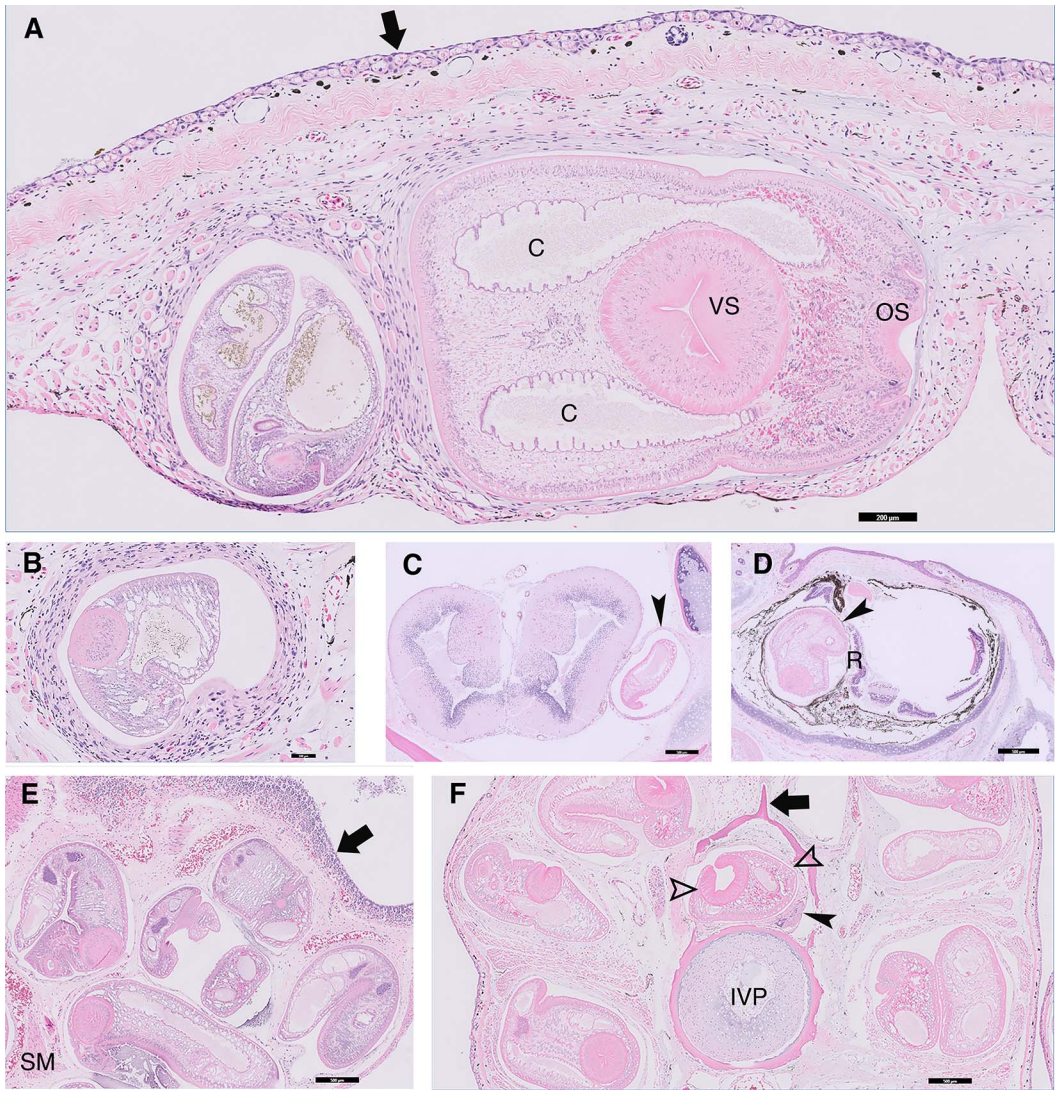

FIGURE 4. Histopathology of metacercariae in *Ambystoma tigrinum* from Blue Stem Connector Pond in Boulder, Colorado, USA. (A) Two metacercariae embedded in the body wall of a female tiger salamander. The larger profile is surrounded by a thin layer of myxomatous matrix and scant encapsulation. The smaller profile is surrounded by denser collagenous encapsulation; C = paired ceca, VS = ventral sucker, OS = oral sucker, arrow = skin surface of the salamander. (B) Although most metacercariae were surrounded by a poorly cellular myxomatous matrix, few parasites were encapsulated by variable numbers of granulocytes, lymphocytes, macrophages, rare multinucleate giant cells, and fibroblasts. (C) A metacercaria (arrowhead) is present between the brain and calvarium. (D) A metacercaria (arrowhead) is present in the eye in the choroid; R = retina. (E) Five metacercariae encysted in the submucosa of the stomach with minimal surrounding tissue reaction. Arrow = gastric mucosa, SM = smooth muscle of gastric wall. (F) Cross section through the decalcified tail of a female tiger salamander showing several metacercaria in the skeletal muscle, with one in the vertebral canal causing severe compression of the spinal cord; IVP = intervertebral pad, arrow = dorsal spinous process of the vertebra, arrowhead = compressed spinal cord. All H&E.

parasites encysted in the pulmonary pleura, epicardium, or other serosal surfaces. Encysted metacercariae were detected in the spinal canal in 2/4 sections of the spine from each animal. At these sites, the metacercariae caused marked compression and lateral deviation of the spinal cord (Fig. 4C). In one salamander, a solitary metacercaria was detected in the choroid of the eye in association with retinal detachment while another metacercaria was found in the calvarium. Each metacercaria had a ridged tegument, solid parenchyma with muscle fibers, and a single ventral large muscular sucker (~600–670 μm diameter) and a smaller anterior oral sucker (~250–270 μm). The metacercariae had bilateral intestinal ceca, and both male and female reproductive tracts. Each parasitic organism was flanked by 30–200 μm of concentrically arranged fibroplasia that ranged from poorly cellular and myxomatous (probably early lesion, Fig. 4A, right) to moderately cellular and collagenous (later-stage lesion, Fig. 4A, right and Fig. 4D). Embedded in this matrix layer were low to modest numbers of melanocytes and low numbers of granulocytes. Fewer than 1% of all cysts were ruptured or degenerate; these were surrounded by modest to high numbers of granulocytes, mononuclear cells, few multinucleated giant cells, mild local hemorrhage, and erythrophagic and pigment-laden macrophages (Fig. 4E, F).

Video processing

We recorded videos of 62 *A. tigrinum* collected from Blue Stem Connector Pond in 2022–2023. Of those, 58 (93.5%) were usable; the others were either corrupted or could not be analyzed (because of unstable footage or insufficient coverage of the salamander), and were removed from the data set. Of the usable videos, 15.5% of examined *A. tigrinum* exhibited no obvious cysts or nodules; the remaining videos exhibited 1–424 (median 39) externally visible cysts per animal. For the 23 salamanders that were assessed by video then necropsied, there was a strongly positively correlation (r=0.81; 95% confidence interval [CI], 0.72–0.88) between the number of cysts observed on video and the counts determined during necropsy. The functional relationship between video counts and necropsy counts was best captured by including both a linear and quadratic term for video counts in predicting necropsy load (negative binomial GLM; scaled[VideoCount]=2.7 ± 0.4, $z = 7.6$, $P<0.0000001$; scaled[VideoCount^2] = -1.4 ± 0.3, $z = -4.3$, $P < 0.00001$; Fig. 5A). Thus, counts of cysts on videos were a positive predictor of *C. marginatum* metacercariae loads, although this relationship weakened as loads became extremely high (past 250 video-counted cysts and 1,500 metacercariae recorded during necropsy). Actual loads of metacercariae from necropsy were always higher than video-based counts, owing in part to the abundance of parasites in tissues not externally visible. All 11 uninfected hosts were correctly classified as cyst-free based on video assessment and later necropsy. For the 58 salamanders in which videos were assessed by two independent reviewers (n=58), the correlation between reviewers was 0.90 (95% CI = 0.84–0.94, $P<0.00001$), indicating that reviewer counts were broadly consistent (Fig. 5B).

DISCUSSION

Our investigation of this morbidity event affecting tiger salamanders (*A. tigrinum*) detected extremely heavy loads of *C. marginatum.* These levels may be among the highest infection levels ever reported in amphibians, with up to 4,075 metacercariae per host and a mean intensity of $1,203 \pm 224$ SE among salamanders across both years. Mean and maximum loads of *Clinostomum* metacercariae in amphibians are generally much lower, ranging from 6 to 44 (see Calhoun et al. 2019; McAllister et al. 2023). Based on previous measurements of the per-metacercaria wet mass of *C. marginatum* (1.05 mg; see Lambden and Johnson 2013), we estimate that the combined clinostomid mass within these salamanders was mean 3,328 mg, or approximately 4.1–5.5% of the animals' total wet mass. Usually, both prevalence and infection load of these

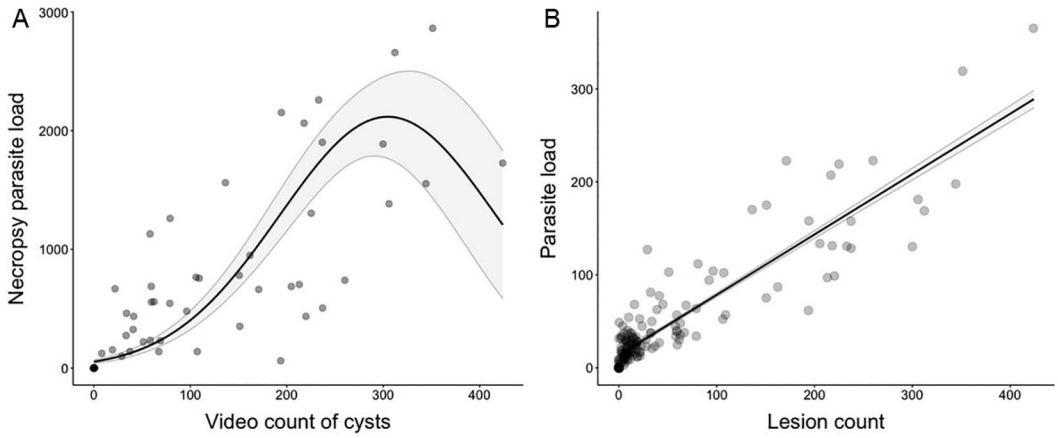

FIGURE 5. (A) Relationship between counts of *Clinostomum marginatum* metacercariae during necropsy and the number of externally evident cysts detected on videos. Results indicate a significant, nonlinear relationship between the two variables (scaled[VideoCount] = 2.7 ± 0.4, z = 7.6, $P<0.00001$) up to a certain load found in necropsy, where the quadratic model indicates a decrease (scaled[VideoCount^2] = 1.4 ± 0.3, z = −4.3, $P<0.00001$). (B) Correlation between two independent reviewers scoring 58 videos of salamanders and their cyst counts observed on video. Results indicated a strongly positive correlation of 0.90 (95% confidence interval = 0.84–0.94, $P<0.00001$).

trematodes in amphibians are low. In the Southern Great Plains of North America, external assessment of >64,000 individuals detected only 0.4% of three amphibian species infected with *Clindostomum attenuatum* (Gray et al. 2007). Similarly, a study of 12,360 amphibian hosts in the Bay Area of California reported an overall *C. marginatum* infection prevalence of 1.7% with a maximum load of 44 (Calhoun et al. 2019), whereas Green et al. (2002) reviewing 64 amphibian morbidity and mortality events in the US submitted to National Wildlife Health Center in Madison, Wisconsin, US, 1996–2001 found only six cases of dermal *Clinostomum* spp. infection associated with morbidity.

Interestingly, we saw a sharp decline in *C. marginatum* infection in 2023, in which 22% of animals exhibited infection. In situ field observations indicated that severely infected animals exhibited lethargy and improper buoyancy, and histological assessments suggested that the heavy loads of *C. marginatum* caused localized inflammation in a range of host tissues. Such infections might affect both survival and development. Based on their increased relative size, we suspect that the individuals found infected in 2023 had probably been exposed in 2022 and had overwintered as larvae. Overwintering has been documented in *Ambystoma* spp. previously (Ireland 1973; Phillips 1992; Pearson 2004). Delayed metamorphosis has been reported in other amphibian hosts supporting high infection loads of trematodes (Johnson et al. 2006; Johnson and Hartson 2009; Orlofske et al. 2017).

Histologic findings provided additional insights into the nature of the infections beyond what was evident during necropsy. For example, metacercariae were identified histologically in the spinal canal, calvarium, and eye. *Clinostomum* spp. have been previously reported to cause ocular, muscular, and spinal pathology in *A. tigrinum* (Perpiñán et al. 2010). Ocular cysts could result in significant impairment by decreasing a host's ability to detect prey visually and evade predation, and cysts in the spinal canal could lead to paresis or paralysis.

There are more than 10 nominal species of *Clinostomum* in North America, with *Clinostomum complanatum*, *C. attenuatum*, and *C. marginatum* reported in amphibians. (Calhoun et al. 2019). Based on DNA sequences, the trematodes obtained in our study were *C. marginatum*, *R. ondatrae*, and *Ce. americanus*.

The collected *C. marginatum* and *R. ondatrae* samples were metacercariae, whereas *Ce. americanus* included metacercariae and adults. As an adult, *Ce. americanus* is an intestinal parasite of amphibians, which become infected by consuming metacercariae encysted in either their own skin or that of other consumed amphibians. Morphological identifications based on larval morphology alone are often unreliable, but the new DNA sequences matched those in GenBank from morphologically identified adults. The detection of *R. ondatrae*, *Ce. americanus*, and *M. elongata* from Colorado tiger salamanders are consistent with previous reports (Adamson and Richardson 1989; Johnson et al. 2004; Perpiñán et al. 2010). *Ribeiroia ondatrae*, a digenetic trematode using planorbid snails as a first intermediate host, fish and amphibians as second intermediate hosts, and piscivorous birds or mammals as definitive hosts, is known to cause limb malformations in amphibians (Johnson et al. 2004). Most recently, *R. ondatrae* was the suspected agent of mortality in threatened or endangered salamanders (*Ambystoma californiense* and *Ambystoma macrodactylum croceum*) in the Ellicott National Wildlife Refuge in Santa Cruz, California (Keller et al. 2021). Nevertheless, we did not see any mortality associated with this infection in these salamander larvae. Colorado is a new geographical location of record for *M. elongata*, which has been previously reported in *A. tigrinum* from Mexico and as far north as Utah (Adamson and Richardson 1989; Dinger et al. 2005).

One way to minimize sampling impact on vulnerable populations of wildlife animal is to use noninvasive techniques to evaluate disease. Our analysis of videographic data indicated a high agreement between cysts quantified on animals in the field using video and formal quantification of metacercariae during necropsy. The best-fitting model was nonlinear, with the noninvasive approach starting to become less accurate as infection loads reach very high levels. Because more than 50% of *C. marginatum* metacercariae occur internally within the host, cyst counts estimated by external video were invariably lower than necropsy, yet nonetheless provided reliable evidence for detection and an approximation of infection load intensity. Moreover, independent reviewers generated highly concordant assessments of cyst counts across 35 animals, yielding a correlation coefficient of 0.90. These results indicate that, with proper training, this method of video analysis can be used to estimate an obvious infection such as that seen in this epizootic, potentially creating opportunities for low-impact disease monitoring by biologists or trained members of the public. The incorporation of community science in wildlife health surveillance can be beneficial, particularly where resources are limited and cost effectiveness is paramount; however, careful training in animal handling is necessary (Lawson et al. 2015; McKinley et al. 2017). This technique could be also applied to other similar parasite infections that present visually on their hosts (De Wit and Johnson 2024).

It is unclear why infection levels in 2022 were so extreme. We are not aware of other such epizootics in tiger salamanders from Colorado, and extensive previous surveys of lentic-breeding amphibians in the Front Range have not detected such events (e.g., Johnson et al. 2011, 2013; P.T.J.J. pers. obs.). Whether the high infection loads inhibited or delayed metamorphosis is also unclear, but could warrant additional investigation. For instance, infection by other trematodes, such as *R. ondatrae*, has often been found to delay time to metamorphosis (Johnson et al. 2012). Based on the design of the study and its observational nature, we were not able to test the consequences of the high infection loads for host behavior, survival, and morbidity directly. Nonetheless, to discern the true impact of such high metacercarial burdens on tiger salamander, future work may include experimental studies wherein behavioral changes and changes in growth, weight gain, or time to metamorphosis could be assessed following infection with different parasite loads under controlled conditions. Given the small size of Blue Stem Connector Pond (about 253.50 m^2) and the fact that 2022 was a relatively hot and dry year (US Department of

Agriculture, 2022), the origin of the epizootic might have resulted from unusual activity of the avian definitive hosts and strong growth conditions for snail intermediate hosts. Sustained activity around the pond by a heavily infected definitive host) could enhance the density of infected snails (e.g., *Helisoma trivolvis*, which are common in the pond), leading to high transmission to larval salamanders. Whether such activity by bird hosts was a stochastic event or perhaps linked to movement of migratory birds into the Intermountain West in response to severe drought conditions along the Pacific Flyway is unknown. Further sampling into the future will be required to evaluate potential drivers as well as the consequences of infection for this species and for other amphibian species, including state species of conservation importance such as the northern leopard frog (*Rana pipiens*), that also use this pond and others in the area.

ACKNOWLEDGMENTS

First and foremost, we thank our field collection team (Sophie Elliot, Forrest Lacey, Macallynn Lacey, Katelyn Johnson, and Kyle Johnson) and our dissection team (Jamie Curtis, Rachel Seyler, and Natalie Pelton). We also thank William Keeley and Boulder OSMP for continued access and support of our research. We thank Emily Barker and the University of Colorado Museum of Natural History for accepting voucher specimens into the collection. Additionally, we thank John Michael Kinsella for identification of *Megalobatrachonema elongata* and Easton Klein for assistance with video processing. This work was supported by OSMP (OSMP Funded Research Program 2023 [23HP529] respectively), an Undergraduate Research Opportunity grant (University of Colorado), and a University System of Georgia Stem Initiative IV grant (awarded to Middle Georgia State University). Finally, we thank three reviewers and the editor for their comments to improve the manuscript.

LITERATURE CITED

Adamson ML, Richardson JPM. 1989. Historical biogeography and host distribution of *Chabaudgolvania* spp., nematode parasites of salamanders. *J Parasitol Res* 75:892–897.

Albon SD, Stien A, Irvine RJ, Langvatn R, Ropstad E, Halvorsen O. 2002. The role of parasites in the dynamics of a reindeer population. *Proc Biol Sci* 269:1625–1632.

Becker CG, Rodriguez D, Lambertini C, Toledo LF, Haddad CFB. 2016. Historical dynamics of *Batrachochytrium dendrobatidis* in Amazonia. *Ecography* 39:954–960.

Blaustein AR, Gervasi SS, Johnson PTJ, Hoverman JT, Belden LK, Bradley PW, Xie GY. 2012. Ecophysiology meets conservation: Understanding the role of disease in amphibian population declines. *Philos Trans R Soc Lond B* 367:1688–1707.

Bosch J, Thumsová B, López-Rojo N, Pérez J, Alonso A, Fisher MC, Boyero L. 2021. Microplastics increase susceptibility of amphibian larvae to the chytrid fungus *Batrachochytrium dendrobatidis*. *Sci Rep* 11:22438.

Bower DS, Brannelly LA, McDonald CA, Webb RJ, Greenspan SE, Vickers M, Gardner MG, Greenlees MJ. 2019. A review of the role of parasites in the ecology of reptiles and amphibians. *Aust J Ecol* 44:433–448.

Brooks ME, Kristensen K, van Benthem KJ, Magnusson A, Berg CW, Nielsen A, Skaug HJ, Mächler M, Bolker BM. 2017. glmmTMB balances speed and flexibility among packages for zero-inflated generalized linear mixed modeling. *R Journal* 9:378–400.

Bush AO, Lafferty KD, Lotz JM, Shostak AW. 1997. Parasitology meets ecology on its own terms: Margolis et al. revisited. *J Parasitol Res* 83:575–583.

Caffara M, Locke SA, Gustinelli A, Marcogliese DJ, Fioravanti ML. 2011. Morphological and molecular differentiation of *Clinostomum complanatum* and *Clinostomum marginatum* (Digenea: Clinostomidae) metacercariae and adults. *J Parasitol* 97:884–891.

Calhoun DM, Leslie KL, Riepe TB, Achatz TJ, McDevitt-Galles T, Tkach VV, Johnson PTJ. 2019. Patterns of *Clinostomum marginatum* infection in fishes and amphibians: Integration of field, genetic, and experimental approaches. *J Helminthol* 94:e44.

Daszak P, Cunningham AA, Hyatt AD. 2003. Infectious disease and amphibian population declines. *Divers Distrib* 9:141–150.

De Wit CDG, Johnson PTJ. 2024. Black Spot Syndrome in ocean surgeonfish: Using video-based surveillance to quantify disease severity and test environmental drivers. *Mar Biol* 171:110–120.

Dinger EC, Cohen AE, Hendrickson DA, Marks JC. 2005. Aquatic invertebrates of Cuatro Ciénegas, Coahuila, México: Natives and exotics. *Southwest Nat* 50:237–246.

DiRenzo GV, Campbell Grant EH, Longo AV, Che-Castaldo C, Zamudio KR, Lips KR. 2018. Imperfect pathogen detection from non-invasive skin swabs biases disease inference. *Methods Ecol Evol* 9:380–389.

Duffus ALJ, Waltzek TB, Stöhr AC, Allender MC, Gotesman M, Gray MJ, Grayfer L, Hick P, Hines MK, et al. 2015. Distribution and host range of ranaviruses. In: *Ranaviruses: Lethal pathogens of ectothermic vertebrates*, Gray MJ, Chinchar VG, editors. Springer, New York, New York, pp. 9–57.

Everest DJ, Tolhurst-Cherriman DAR, Davies H, Dastjerdi A, Ashton A, Blackett T, Meredith AL, Milne E, Mill A, Shuttleworth CM. 2019. Assessing a potential non-invasive method for viral diagnostic purposes in European squirrels. *Hystrix* 30:44–50.

Gibson DI, Jones A, Bray RA. 2002. *Keys to the Trematoda*. CABI, London, UK.

Goater CP, Semlitsch RD, Bernasconi MV. 1993. Effects of body size and parasite infection on the locomotory performance of juvenile toads, *Bufo bufo*. *Oikos* 66:129–136.

Goater CP, Vandenbos RE. 1997. Effects of larval history and lungworm infection on the growth and survival of juvenile wood frogs (*Rana sylvatica*). *Herpetologica* 53:331–338.

Goater CP, Ward P. 1992. Negative effects of *Rhabdias bufonis* (Nematoda) on the growth and survival of toads (*Bufo bufo*). *Oecologia* 89:161–165.

Gray MJ, Miller DL, Hoverman JT. 2009. Ecology and pathology of amphibian ranaviruses. *Dis Aquat Organ* 87:243-266.

Gray MJ, Smith LM, Miller DL, Bursey CR. 2007. Influences of agricultural land use on *Clinostomum attenuatum* metacercariae prevalence in southern Great Plains amphibians. *Herpetol Conserv Biol* 2:23–28.

Green DE, Converse KA, Schrader AK. 2002. Epizootiology of sixty-four amphibian morbidity and mortality events in the USA, 1996–2001. *Ann N Y Acad Sci* 969:323–339.

Hall EM, Goldberg CS, Brunner JL, Crespi EJ. 2018. Seasonal dynamics and potential drivers of ranavirus epidemics in wood frog populations. *Oecologia* 188:1253–1262.

Harrison RG. 1969. Stages and description of the normal development of the spotted salamander, *Ambystoma punctatum* (Linn.). In: *Organization and development of the embryo*, Harrison RG, Willens S, eds. Yale University Press, New Haven, Connecticut, pp. 44–66.

Herczeg D, Ujszegi J, Kásler A, Holly D, Hettyey A. 2021. Host–multiparasite interactions in amphibians: A review. *Parasit Vectors* 14:296–316.

Hoffman GL. 1999. *Parasites of North American freshwater fishes*. Cornell University Press, Ithaca, New York.

Hudson P, Greenman J. 1998. Competition mediated by parasites: Biological and theoretical progress. *Trends Ecol Evol* 13:387–390.

Huver J, Koprivnikar J, Johnson PTJ, Whyard S. 2015. Development and application of an eDNA method to detect and quantify a pathogenic parasite in aquatic ecosystems. *Ecol Appl* 25:991–1002.

Ireland PH. 1973. Overwintering of larval spotted salamanders, *Ambystoma maculatum* (Caudata) in Arkansas. *Southwest Nat* 17:435–437.

Johnson PTJ, Calhoun DM, Riepe T, McDevitt-Galles T, Koprivnikar J. 2019. Community disassembly and disease: Realistic—but not randomized—biodiversity losses enhance parasite transmission. *Proc Biol Sci* 286:20190260.

Johnson PTJ, Calhoun DM, Stokes AN, Susbilla CB, McDevitt-Galles T, Briggs CJ, Hoverman JT, Tkach VV, de Roode JC. 2018. Of poisons and parasites—The defensive role of tetrodotoxin against infections in newts. *J Anim Ecol* 87:1192–1204.

Johnson PTJ, Hartson RB. 2009. All hosts are not equal: Explaining differential patterns of malformations in an amphibian community. *J Anim Ecol* 78:191–201.

Johnson PTJ, Kellermanns E, Bowerman J. 2011. Critical windows of disease risk: Amphibian pathology driven by developmental changes in host resistance and tolerance. *Funct Ecol* 25:726–734.

Johnson PTJ, Preston DL, Hoverman JT, Richgels KLD. 2013. Biodiversity decreases disease through predictable changes in host community competence. *Nature* 494:230–300.

Johnson PTJ, Preu ER, Sutherland DR, Romansic JM, Han B, Blaustein AR. 2006. Adding infection to injury: Synergistic effects of predation and parasitism on amphibian malformations. *Ecology* 87:2227–2235.

Johnson PTJ, Rohr JR, Hoverman JT, Kellermanns E, Bowerman J, Lunde KB. 2012. Living fast and dying of infection: Host life history drives interspecific variation in infection and disease risk. *Ecol Lett* 15:235–242.

Johnson PTJ, Sutherland DR, Kinsella J, Lunde KB. 2004. Review of the trematode genus *Ribeiroia* (Psilostomidae): Ecology, life history, and pathogenesis with special emphasis on the amphibian malformation problem. *Adv Parasitol* 57:191–253.

Keller S, Roderick CL, Caris C, Grear DA, Cole RA. 2021. Acute mortality in California tiger salamander (*Ambystoma californiense*) and Santa Cruz long-toed salamander (*Ambystoma macrodactylum croceum*) caused by *Ribeiroia ondatrae* (Class: Trematoda). *Int J Parasitol Parasites Wildl* 16:255–261.

Kolby JE, Smith KM, Ramirez SD, Rabemananjara F, Pessier AP, Brunner JL, Goldberg CS, Berger L, Skerratt LF. 2015. Rapid response to evaluate the presence of amphibian chytrid fungus *(Batrachochytrium dendrobatidis)* and ranavirus in wild amphibian populations in Madagascar. *PLoS One* 10:e0125330.

Koprivnikar J, Marcogliese DJ, Rohr JR, Orlofske SA, Raffel TR, Johnson PTJ. 2012. Macroparasite infections of amphibians: What can they tell us? *Ecohealth* 9:342–360.

Lambden J, Johnson PTJ. 2013. Quantifying the biomass of parasites to understand their role in aquatic communities. *Ecol Evol* 3:2310–2321.

Lawson B, Petrovan SO, Cunningham AA. 2015. Citizen science and wildlife disease surveillance. *Ecohealth* 12:693–702.

Lehmann DL. 1954. Some helminths of west coast urodeles. *J Parasitol* 40:231–232.

Littlewood DTJ, Olson PD. 2014. Small subunit rDNA and the Platyhelminthes: Signal, noise, conflict and compromise. In: *Interrelationships of the Platyhelminthes*, Littlewood DTJ, Bray RA, editors. CRC Press, New York, New York, pp. 262–278.

Luikart G, Ezenwa V, Kardos M, White PJ, Cross P. 2006. Predicting disease spread in Greater Yellowstone ungulates using parasite DNA markers. In: *University of Wyoming National Park Service Research Center 30th Annual Report*, Wyoming Scholars Repository, Laramie, Wyoming, pp. 119–122.

McAllister CT. 1990. *Metacercaria of Clinostomum complanatum* (Rudolphi, 1814) (Trematoda: Digenea) in a Texas salamander, *Eurycea neotenes* (Amphibia: Caudata), with comments on *C. marginatum* (Rudolphi, 1819). *J Helminthol Soc Wash* 57:69–71.

McAllister CT, Fenolio DB, Slay ME, Cloutman DG. 2023. First parasites (Cnidaria: Myxobolidae; Trematoda: Digenea: Clinostomidae) reported from the

threatened Ozark cavefish, *Troglichthys rosae* (Percopsiformes: Amblyopsidae), from Arkansas, USA, with a summary of the parasites of North American cavefishes. *Comp Parasitol* 90:73–77.

McKinley DC, Miller-Rushing AJ, Ballard HL, Bonney R, Brown H, Cook-Patton SC, Evans DM, French RA, Parrish JK, et al. 2017. Citizen science can improve conservation science, natural resource management, and environmental protection. *Biol Conserv* 208:15–28.

Moretti EH, Madelaire CB, Silva RJ, Mendonça MT, Gomes FR. 2014. The relationships between parasite intensity, locomotor performance, and body condition in adult toads (*Rhinella icterica*) from the wild. *J Herpetol* 48:277–283.

Olson DH, Aanensen DM, Ronnenberg KL, Powell CI, Walker SF, Bielby J, Garner TWJ, Weaver G, Bd Mapping Group, Fisher MC. 2013. Mapping the global emergence of *Batrachochytrium dendrobatidis*, the amphibian chytrid fungus. *PloS One* 8:e56802.

Orlofske SA, Belden LK, Hopkins WA. 2017. Effects of *Echinostoma trivolvis* metacercariae infection during development and metamorphosis of the wood frog (*Lithobates sylvaticus*). *Comp Biochem Physiol Part A Mol Integr Physiol* 203:40–48.

Pearson KJ. 2004. The effects of introduced fish on the long-toed salamander (*Ambystoma macrodactylum*) in southwestern Alberta, Canada. Ph.D. Thesis, Faculty of Arts and Science, University of Lethbridge, Alberta, Canada, 200 pp.

Perpiñán D, Garner MM, Trupkiewicz JG, Malarchik J, Armstrong DL, Lucio-Forster A, Bowman DD. 2010. Scoliosis in a tiger salamander (*Ambystoma tigrinum*) associated with encysted digenetic trematodes of the genus *Clinostomum*. *J Wildl Dis* 46:579–584.

Phillips CA. 1992. Variation in metamorphosis in spotted salamanders *Ambystoma maculatum* from eastern Missouri. *Am Midl Nat* 128:276–280.

R Core Team. 2022. R: A language and environment for statistical computing. Vienna: R Foundation for Statistical Computing, Vienna, Austria. http://www.R-project.org. Accessed November 2024.

Razo-Mendivil U, de León GPP. 2011. Testing the evolutionary and biogeographical history of *Glypthelmins* (Digenea: Plagiorchiida), a parasite of anurans, through a simultaneous analysis of molecular and morphological data. *Mol Phylogenet Evol* 59:331–341.

Scheele BC, Foster CN, Hunter DA, Lindenmayer DB, Schmidt BR, Heard GW. 2019. Living with the enemy: Facilitating amphibian coexistence with disease. *Biol Conserv* 236:52–59.

Schell SC. 1985. *Handbook of Trematodes of North America north of Mexico*. University of Idaho Press, Moscow, Idaho.

Schilling AK, Mazzamuto MV, Romeo C. 2022. A review of non-invasive sampling in wildlife disease and health research: What's new? *Animals (Basel)* 12:1719.

Snyder SD, Tkach VV. 2007. *Neosychnocotyle maggiae*, n. gen., n. sp. (Platyhelminthes: Aspidogastrea) from freshwater turtles in northern Australia. *J Parasitol Res* 93:399–403.

Standish I, Leis E, Schmitz N, Credico J, Erickson S, Bailey J, Kerby J, Phillips K, Lewis T. 2018. Optimizing, validating, and field testing a multiplex qPCR for the detection of amphibian pathogens. *Dis Aquat Organ* 129:1–13.

Tkach V, Pawlowski J. 1999. A new method of DNA extraction from the ethanol-fixed parasitic worms. *Acta Parasitol* 44:147–148.

Tkach VV, Kudlai O, Kostadinova A. 2016. Molecular phylogeny and systematics of the Echinostomatoidea Looss, 1899 (Platyhelminthes: Digenea). *Int J Parasitol* 46:171–185.

Tkach VV, Littlewood DTJ, Olson PD, Kinsella JM, Swiderski Z. 2003. Molecular phylogenetic analysis of the Microphalloidea Ward, 1901 (Trematoda: Digenea). *Syst Parasitol* 56:1–15.

US Department of Agriculture. 2022. Drought conditions in Western States in summers of 2021, 2022 were the most intense in 20 years. https://www.ers.usda.gov/data-products/chart-gallery/gallery/chart-detail/?chartId=104849. Accessed February 2025.

Wilber MQ, Briggs CJ, Johnson PTJ. 2020. Disease's hidden death toll: Using parasite aggregation patterns to quantify landscape-level host mortality in a wildlife system. *J Anim Ecol* 89:2876–2887.

Submitted for publication 25 April 2024.
Accepted 12 December 2024.